Published in final edited form as:
Circ Res. 2020 December 04; 127(12): 1522–1535. doi:10.1161/CIRCRESAHA.120.317054.

Genome-Wide Analysis Identifies an Essential Human TBX3 Pacemaker Enhancer.

Vincent W.W. van Eif[1], **Stephanie Protze**[2], **Fernanda M. Bosada**[1], **Xuefei Yuan**[3,8], **Tanvi Sinha**[4], **Karel van Duijvenboden**[1], **Auriane C. Ernault**[5,6], **Rajiv A. Mohan**[1], **Vincent Wakker**[1], **Corrie de Gier-de Vries**[1], **Ingeborg B. Hooijkaas**[1], **Michael D. Wilson**[3,8], **Arie O. Verkerk**[1,5], **Jeroen Bakkers**[7], **Bastiaan J. Boukens**[1,5], **Brian L. Black**[4], **Ian C. Scott**[3,8], **Vincent M. Christoffels**[1,*]

1)Department of Medical Biology, Amsterdam Cardiovascular Sciences, Amsterdam University Medical Centers, University of Amsterdam, Amsterdam, The Netherlands 2)McEwen Stem Cell Institute, University Health Network and the Department of Molecular Genetics, University of Toronto, Toronto, Ontario, Canada 3)The Hospital for Sick Children; and the Department of Molecular Genetics, University of Toronto, Toronto, Ontario, Canada 4)Cardiovascular Research Institute, Department of Biochemistry and Biophysics, University of California, San Francisco, United States 5)Department of Experimental Cardiology, University of Amsterdam, Amsterdam University Medical Centers, Amsterdam, The Netherlands 6)Aix-Marseille Université, INSERM, MMG - U1251, Marseille, France 7)Hubrecht Institute and University Medical Center Utrecht, 3584 CT Utrecht, Netherlands. 8)Department of Molecular Genetics, University of Toronto, Canada

Abstract

Rationale: The development and function of the pacemaker cardiomyocytes of the sinoatrial node (SAN), the leading pacemaker of the heart, are tightly controlled by a conserved network of transcription factors, including TBX3, ISL1 and SHOX2. Yet, the regulatory DNA elements (REs) controlling target gene expression in the SAN pacemaker cells have remained undefined.

Objective: Identification of the regulatory landscape of human SAN-like pacemaker cells and functional assessment of SAN-specific REs potentially involved in pacemaker cell gene regulation.

Methods and results: We performed ATAC-seq on human pluripotent stem cell-derived SAN-like pacemaker cells and ventricle-like cells and identified thousands of putative regulatory DNA elements specific for either human cell type. We validated pacemaker cell-specific elements in the *SHOX2* and *TBX3* loci. CRISPR-mediated homozygous deletion of the mouse orthologue of a noncoding region with candidate pacemaker-specific REs in the *SHOX2* locus resulted in selective loss of *Shox2* expression from the developing SAN and embryonic lethality. Putative pacemaker-specific REs were identified up to 1 Mbp upstream of *TBX3* in a region close to *MED13L* harboring variants associated with heart rate recovery after exercise. The orthologous region was deleted in mice, which resulted in selective loss of expression of *Tbx3* from the SAN and (cardiac)

*Correspondence to v.m.christoffels@amsterdamumc.nl.

Disclosures
None

ganglia and in neonatal lethality. Expression of *Tbx3* was maintained in other tissues including the atrioventricular conduction system, lungs, and liver. Heterozygous adult mice showed increased SAN recovery times after pacing. The human REs harboring the associated variants robustly drove expression in the SAN of transgenic mouse embryos.

Conclusions: We provided a genome-wide collection of candidate human pacemaker-specific REs, including the loci of *SHOX2*, *TBX3* and *ISL1*, and identified a link between human genetic variants influencing heart rate recovery after exercise and a variant RE with highly conserved function, driving SAN expression of *TBX3*.

Keywords

Sinoatrial node; regulatory element; functional assessment; GWAS; heart rate recovery time

Introduction

Rhythmic contractions of the heart are dictated by the sinoatrial node (SAN), the leading pacemaker of the heart. SAN dysfunction may result in bradycardia requiring implantation of an electronic artificial pacemaker.[1] The SAN is a complex heterogeneous structure composed of different cell types.[1] The development and function of the pacemaker cardiomyocytes of the SAN relies on a balanced gene regulatory network, tightly controlled by transcription factors (TFs) that act in tissue, stage and dose-dependent manners.[2, 3] Multiple TFs essential for pacemaker cell development and function have been identified, including ISL1, SHOX2 and TBX3.[4–7] Activation or inhibition of gene transcription is controlled by tissue-specific and common TFs and cofactors that interact with regulatory DNA elements (REs), such as enhancers.[8, 9] While the transcriptomes of the cells of the SAN region of mouse and human have been studied,[4, 10–13] the transcriptional and epigenetic mechanisms underlying the regulation of these SAN genes has remained largely unexplored.

Cardiac epigenetic datasets have allowed for the identification of REs for the human heart[14, 15] but not its smaller components such as the SAN. The pacemaker cells of the SAN are derived from a progenitor cell pool that is different from the cell population contributing to the other components of the heart, and their differentiation is regulated by different TFs and signaling pathways.[2, 3, 16] Therefore, the transcriptional regulatory mechanisms and REs functioning in the SAN are likely to be distinct from those of the rest of the heart. Epigenetic datasets specific for the (human) SAN that would enable SAN-specific RE identification are currently lacking. Recently, different strategies have been described to generate pacemaker cells *in vitro* from human pluripotent stem cells that could function as biological pacemakers.[17, 18] The use of cultured human cells could overcome technical and ethical challenges, and provide valuable epigenetic data facilitating the analysis of human pacemaker-specific gene regulatory mechanisms.

Here, we identified putative pacemaker REs and TF binding motifs in human pluripotent stem cell-derived pacemaker and ventricle-like cells[18] and validated the function of several RE candidates in the loci close to *SHOX2, ISL1* and *TBX3* in transgenic mice and zebrafish.

Moreover, we identified a SAN-specific RE in the region 1 Mbp distal from *TBX3*, which contains a variant associated with heart rate recovery after exercise (HRRAE).[19, 20]

Methods

More detailed Methods are available in the Online Supplement.

Ethics statement

Animal care and experiments (mouse) were in accordance with national and institutional guidelines and approved nationally by the Central Committee Animal Experiments (CCD) and institutionally by the Institution of Animal Welfare (IvD) of Amsterdam UMC, location AMC or were approved by the University of California, San Francisco Institutional Animal Care and Use Committee and complied with all federal and institutional guidelines. Zebrafish were maintained and handled under the guidance and approval of the Canadian Council on Animal Care and the Hospital for Sick Children Laboratory Animal Services.

Cell culture and ATAC-sequencing

The HES3-Nkx2–5$^{gfp/w}$ human embryonic stem cell line[21] was cultured and differentiated towards SANLPC and VLCM and purified as described previously.[18] ATAC-seq was performed on purified cells from three independent differentiations. Nuclei isolation, transposase reaction, washing and amplification procedures have been described earlier.[22] Samples were sequenced on a HiSeq 2500 sequencer (Illumina) using 125 bp single-end reads.

ECG, SAN recovery time and AF inducibility in adult mice

Male and female mice were used. Mice were anaesthetized using 5% isoflurane, and after disappearance of reflexes mice were placed on temperature fixed mat with a steady flow of 1.5% isoflurane. Electrodes were inserted subcutaneously in the limbs and connected to an ECG amplifier (Powerlab 26T, AD Instruments). ECG was measured for 5 minutes before further pacing experiments. ECG parameters were determined from the last minute of a 5 minute recording. Heart rate variation (HRV) was determined by calculating the standard deviation of all RR intervals used to obtain the average reported RR. Pacing studies were performed and atrial arrhythmia inducibility was determined as detailed in the Online Methods. The experimenters were blind to mouse genotype during measurements and outcome assessment.

Data availability

ATAC-seq datasets have been deposited under GEO accession number GSE146044.

Statistics

Mann-Whitney U tests were used for gene expression analysis in Figure 1A, Figure 4B,C (GraphPad Prism 8). Fetal heart rate was statistically analyzed using Kruskal-Wallis test. $P<0.05$ indicates statistical significance (Figure 5A). For ECG parameters before and after ANS block (Figure 5B; Online Fig XIA)), datasets were tested for normality using either Kolmogorov-Smirnoff tests, and were statistically tested using repeated measures ANOVA.

Student's t tests were used to compare WT and *MT-280*$^{+/-}$ within each treatment, and paired t tests were used to compare before and after treatment means of each genotype. Welch's correction was used for the SNRT data comparisons that had significantly different variances (GraphPad Prism 8). The Mann-Whitney U test (SigmaStat 3.5) was used for the single cell action potential parameters (Online Fig XID,E). No mathematical correction was made for the multiple statistical tests used across the study.

Results

Epigenetic profiling of human pacemaker-like cells

In order to identify accessible chromatin regions that could serve as regulatory elements (REs) in human pacemaker cells, we performed the Assay for Transposase-Accessible Chromatin using sequencing (ATAC-seq) on SAN-like pacemaker cells (SANLPC) and ventricle-like cardiomyocytes (VLCM), both differentiated from human pluripotent embryonic stem cells (hESC).[18] We first validated marker gene expression in the SANLPC and VLCM cell types, and found expression of pacemaker-specific genes *ISL1*, *TBX3*, *SHOX2, BMP4, HCN4, CACNA2D2, KCNJ3* highly enriched in the SANLPC, whereas marker genes predominantly expressed in (ventricular) chamber cardiomyocytes but at very low levels in pacemaker cells (*NKX2–5*, *IRX4*, *GJA1*, *SCN5A*, *MYL2, MYL7*) enriched in the VLCM population (Figure 1A). To identify tissue-specific REs, peak-calling was performed on ATAC-seq data of SANLPC, VLCM and undifferentiated hESCs.[23] We identified 42k accessible sites in the dataset of SANLPC, 44k in the VLCM and 45k in the hESC of which 12k, 11k and 22k were cell type-specific for the SANLPC, VLCM and undifferentiated hESC datasets, respectively (Figure 1B). We found 29k accessible sites present in both SANLPC and VLCM, whereas comparison of these datasets with undifferentiated hESC yielded 19k and 22k overlapping sites, respectively. This was consistent with the differentiation of the two cell types towards a cardiomyocyte-like phenotype. Furthermore, we compared the SANLPC ATAC-seq data with that of human left atrial (LA) cardiomyocytes[15, 24] and found similar distributions of overlapping and unique accessible sites (Figure 1B).

To identify SANLPC-specific REs, we inspected the locus of *SHOX2*, which is required for SAN development.[5, 6] Multiple DNA regions downstream of *SHOX2* were accessible in SANLPC only (Figure 1C). The SANLPC-selective accessibility was limited to the topologically associating domains (TAD)[25] containing *SHOX2*, as accessibility signals between SANLPC and VLCM were similar in regions adjacent of *SHOX2* (Figure 1C). EMERGE, which merges multiple epigenetic datasets in order to predict locations of REs[15, 26] did not predict cardiac REs in the pacemaker-specific region in the gene desert downstream of *SHOX2*, consistent with the notion that such datasets are generally derived from whole hearts or ventricles.

To gain insight into TFs involved in gene regulation in SANLPCs, VLCMs and undifferentiated hESCs, we performed HOMER motif analysis on cell type-specific accessible sites (Figure 1D). Significant association of motifs for TFs involved in pluripotency (Oct, Sox, Nanog) was detected for hESC-specific sites. SANLPC-specific sites contained motifs for LIM homeobox (Isl1) and T-Box protein (Tbx5, Tbx20) proteins, which are involved in SAN pacemaker cell development and gene regulation.[4, 7, 10, 27] We also detected putative binding sites for TALE homeodomain proteins (Meis1, Tgif1, 2) and Gata factors (Gata3, 4, 6), involved in cardiac cell cycle regulation, cardiac neural crest development and cardiac development, respectively.[28–31] HOMER motif analysis on accessible sites enriched in SANLPC cells compared to LA cardiomyocytes likewise revealed enrichment of motifs for Isl1, T-Box proteins (Tbx5, Eomes, Tbet) and TALE homeodomain proteins (Tgif1, 2, Meis1). In addition, Nanog motifs were enriched, possibly reflecting the immature state of the stem cell derived SANLPCs compared to mature adult LA cardiomyocytes (Figure 1D). We conclude that unique peaks in each dataset are enriched for potential binding sites for TFs that are associated with the differentiation of that particular cell-type *in vivo*.

In vivo validation of SANLPC regulatory element candidates

In accordance with the SANLPC ATAC-seq results, chromatin accessibility profiling of Hcn4$^+$ SAN cells of newborn mice[32] revealed multiple (conserved) accessible regions in the locus of *Shox2* (Figure 2B, Suppl. Fig. IA). To assess whether transcription occurs from the noncoding putative regulatory sequences (i.e. transcription from enhancers), we merged existing transcriptome datasets of mouse right atrium and Hcn4$^+$ SAN cells[10] (Suppl. Fig. II). Transcripts were identified specifically in the SAN tissue from the area downstream of *Shox2*, harboring accessible regions in the genome of ND0 SANs[32] and orthologues of human candidate SANLPC-specific regulatory elements. These data indicate that this region harbors active SAN-specific enhancers.

To investigate the function of the SAN-specific accessible region in the gene desert between *VEPH1* and *SHOX2* (Figure 2A), we deleted an approximately 250-kb homologous region (VS-250) from the mouse genome (Figure 2B). We crossed heterozygous deletion mice and found that homozygous lethality occurred at E11.5 (Suppl. Fig. IIIA). To assess whether homozygous deletion of the noncoding region caused altered *Shox2* expression, we performed immunohistochemistry on wild type and homozygous E10.5 embryos. Analysis of the *Shox2* expression pattern in wild type embryos revealed expression in the limbs but also in the entire sinus venosus and SAN, where *Shox2* was co-expressed with *Hcn4* (Figure 2C; Suppl. Fig. IIIB). In *VS-250*$^{-/-}$ mutants, expression was still observed in the limbs but was depleted from the SAN, venous valves and the sinus venosus (Figure 2C; Suppl. Fig. IIIB). This implies that the VS-250 region harbors REs involved in *Shox2* regulation in the SAN and associated tissues (sinus venosus and venous valves), whereas expression levels in the limbs rely on REs outside the deletion, such as those recently identified in mice[33] (Figure 2B). Although Shox2 was reported to regulate the expression of *Isl1*,[34] *Isl1* expression was maintained in *VS-250*$^{-/-}$ mutant SAN (Figure 2C). Because Shox2 was shown to suppress *Nkx2–5*,[35] we asked whether depletion of Shox2 would cause ectopic activation of Nkx2–5 in the SAN. Wild type embryos exhibit a strict boundary between the Nkx2–5-negative SAN head and Nkx2–5+ SAN tail (Figure 2D), in accordance with previous results.[36, 37] We observed induction of Nkx2–5 expression in the Shox2-negative SAN of E10.5 *VS-250*$^{-/-}$ mutants (Figure 2D). Furthermore, we observed hypoplasia of the SAN (Figure 2C–D) and venous valves (Figure 2D) in *VS-250*$^{-/-}$ mutants. *Shox2* deficient mice die due to severe bradycardia around E11.5,[6] which corresponds to the time of lethality in *VS-250*$^{-/-}$ embryos. We conclude that region VS-250 contains accessible areas in the genome indispensable for the regulation of *Shox2* in the SAN, sinus venosus and venous valves.

To investigate whether SANLPC-specific accessible regions in the *SHOX2* locus represent functional REs, we tested the activity of four human genomic fragments with SANLPC-specific ATAC-seq signals in mice and zebrafish (Figure 2A). *SHOX2-RE1*, *Tg(SHOX2_RE1: GFP)*^{hsc111}, drove expression of GFP in the atrioventricular canal and sinus venosus containing the pacemaker in fish[38, 39] which was confirmed by immunohistochemistry, but we could not detect activity of *SHOX2-RE1* in the SAN of E11.5 mice (Suppl. Fig. IVA,B). However, X-gal staining was observed in the hindbrain and diencephalon, regions associated with *Shox2* expression.[40] *SHOX2-RE2* was restricted to the outflow tract in mice (Suppl. Fig. IVC). In both zebrafish and mice, we could not observe functional activity of *SHOX2-RE3* (Suppl. Fig. IVC). Interestingly, *SHOX2-RE4* was found to be highly conserved in mammals, birds, reptiles and zebrafish (Figure 2E). *SHOX2-RE4, Tg(SHOX2_RE4: GFP)*^{hsc110}, robustly drove GFP expression in the sinus venosus area and neurons of 72 hours post-fertilization (hpf) zebrafish (Figure 2F; Suppl. Fig. IVD) and in the Hcn4^{+}/Shox2^{+} SAN of E11.5 mouse embryos (Figure 2G). We conclude that the *SHOX2* locus harbors at least two REs that are functionally active in the SAN in mice and the pacemaker area in fish.

Next, the *ISL1* locus was inspected and multiple SANLPC-specific accessible regions were identified (Suppl. Fig. VA). We selected three human genomic fragments with SANPLC-specific ATAC-seq signals (*RE1–3*) near *ISL1* that turned out to be functional in zebrafish hearts (Suppl. Fig. VA,F). We detected SAN-enriched non-coding transcripts (enhancer RNAs) in regions up- and downstream of *Isl1* harboring the homologues of both *ISL1-RE1, Tg(ISL1_RE1: GFP)*^{hsc112}, and *ISL1-RE2, Tg(ISL1_RE2: GFP)*^{hsc113}, (Suppl. Fig. VB). Interestingly, *ISL1-RE1* predominantly drove GFP expression in the pacemaker area (sinus venosus) of zebrafish, which was confirmed by immunohistochemistry (Suppl. Fig. VC). In the majority of embryos, *ISL1-RE1* was functionally active in the heart, varying from whole heart GFP expression to the sinus venosus area only (Suppl. Fig. VD). Additionally, we observed activity in neuronal components (Suppl. figure VD). *ISL1-RE2* showed activity in the whole heart (Suppl. Fig. VE) and *ISL1-RE3, Tg(ISL1_RE3: GFP)*^{hsc114}, was consistently active in the brain and heart, although GFP expression patterns in the latter varied from whole heart to inflow tract-specific expression (Suppl. Fig. VF).

Taken together, the SANLPC ATAC-seq reveals regions specifically accessible in pacemaker-like cells, a subset of which represent functional REs active in the mouse SAN or sinus venosus (including pacemaker cells) of fish. These datasets could be useful to further identify human pacemaker REs and gain insight into the gene regulatory network in human pacemaker cells.

Variant genomic region distal from *TBX3* drives expression in SAN and neurons

Tbx3 is involved in SAN development and function.[7] We investigated the *TBX3* locus for the presence of SANLPC REs. Because REs and their target genes are largely confined to the same TAD,[8, 9, 41] Hi-C data[25] were used to identify boundaries of the TAD (Figure 3A).

The TAD structure covers a >1Mbp region in between of *MED13L* and *TBX5*, the neighboring genes of *TBX3*. Previously, REs were identified in relative close proximity to mouse *Tbx3* and showed activity in many sites expressing *Tbx3*, including the atrioventricular canal, His bundle, limbs, mammary glands, body wall, etc., but not in the SAN.[33, 42, 43] Therefore, we hypothesized that SAN REs involved in regulation of TBX3 expression are located more distal to *TBX3*. Genetic variants associated with prolonged HRRAE, a trait possibly linked to SAN function, are located approximately one Mbp from *TBX3*, close to *MED13L* (Figure 3A).[19, 20] However, the SNPs are positioned in the same TAD as *TBX3*, whereas *MED13L* is positioned in the adjacent TAD, suggesting a potential association between HRRAE genetic variants and *TBX3* regulation (Figure 3A). We found multiple SANLPC ATAC-seq peaks (Figure 3A) positioned in close proximity to HRRAE SNPs. In addition, multiple accessible and transcribed sites were identified in mouse SANs in the region orthologous to the human region harboring HRRAE SNPs near *MED13L*, (Suppl. Fig. IB and VI).

To gain insight into the function of the region in the gene desert in-between *MED13L* and *TBX3* harboring the majority of the HRRAE-associated SNPs (Figure 3A), we deleted a 280-kbp homologous region from the mouse genome (*MT-280*) (Suppl. Fig. VI). In addition, the larger region in-between *Med13l* and the previously identified atrioventricular canal and limb REs was removed from the mouse genome, indicated by *MT-550* (Figure 3A; Suppl. Fig. VI). We first crossed heterozygous mutants and found that all genotypes were present in Mendelian ratios in both transgenic lines (*MT-280* and *MT-550*) at prenatal stages (Figure 3B). Furthermore, we found similar survival rates of adult heterozygous mutants and wild type mice (Figure 3B). Although heterozygous mutants were viable and fertile, *MT-280*$^{-/-}$ or *MT-550*$^{-/-}$ mice died at ND0, several hours after birth without any overt morphological heart defects. At birth, *MT-280*$^{-/-}$ and *MT-550*$^{-/-}$ mutants were distinguishable from wild type and heterozygous mice by the absence of a milk spot (Suppl. Fig. VIIA). Therefore, we investigated *MT-280*$^{-/-}$ mutants for cleft palate formation, but could not detect alterations in secondary plate development (Suppl. Fig. VIIB).

We performed immunohistochemistry on E12.5, E17.5 and ND0 mutants in order to investigate changes in spatiotemporal expression patterns of *Tbx3* in the homozygous mutants. In E12.5 *MT-280*$^{-/-}$ and *MT-550*$^{-/-}$ mutants, *Tbx3* was expressed in a pattern highly similar to that of wild type littermates, showing expression in many tissues including neurons, limbs, liver, lungs, esophagus, body wall and the heart (Figure 3C). However, both *MT-280*$^{-/-}$ and *MT-550*$^{-/-}$ mutants specifically lacked expression of *Tbx3* in the SAN (Figure 3C; Suppl. Fig. VIIIA). Although *Tbx3* expression was depleted from the SAN, expression was maintained in the atrioventricular canal, bundle and cushions in E12.5 *MT-280*$^{-/-}$ and *MT-550*$^{-/-}$ mutant mice (Figure 4A; Suppl. Fig. VIIIB). Focusing on *MT-280*, we investigated expression levels of *Tbx3* and adjacent genes in Tbx3^{+} structures using qPCR. *Tbx3* levels were significantly decreased in SAN-containing right atrial tissue samples of E17.5 *MT-280*$^{-/-}$ mutants (Figure 4B), but were not statistically different in liver, lung or limbs. We further quantified expression levels of *Med13l* and *Tbx5*, the neighboring genes of *Tbx3*, in E17.5 SAN/right atrial, lung and limb samples of WT and *MT-280*$^{-/-}$ mutants, but observed no statistical difference in expression levels (Figure 4B; Suppl. Fig. IX). SAN-marker genes *Hcn4* and *Isl1* were still expressed in the SAN of mutants at E12.5, E17.5 and ND0 (Suppl. Fig. VIIIA; Suppl. Fig. XA,B). Quantitative PCR measurements on E17.5 SAN-containing right atrium samples revealed no statistical differences in expression levels of *Isl1*, *Shox2*, *Hcn4*, *Cacna2d2* and *Cacna1g* between WT and *MT-280*$^{-/-}$ mutants (Figure 4C). Collectively, these data reveal the deleted region is selectively required for SAN expression of *Tbx3*, and that Tbx3 expression in the SAN is not required for SAN-specific gene expression.

We observed reduced Tbx3 expression in the dorsal root ganglia (DRG) and sympathetic chains (SC) in *MT-280*$^{-/-}$ E12.5 mutants (Suppl. Fig. XC), which became undetectable at E17.5 (Suppl. Fig. XD). *Tbx3* expression was decreased in E12.5 neuronal cells in the retina as well (Suppl. Fig. XE), but was maintained in the limbs (Suppl. Fig. XE) and lungs (Suppl. Fig. XF). Next, we investigated *Tbx3* expression in the cardiac ganglia that innervate the SAN. At E14.5, we labeled the cardiac ganglia with neuronal marker Tbx3 was absent from the *MT-280*$^{-/-}$ SAN, but was still detectable in the Peripherin-positive cardiac ganglia of E14.5 homozygous mutants (Suppl. Fig. XG). In contrast, at E17.5 Tbx3 was absent from the Isl1^{+}/Actin^{-} cardiac ganglia in *MT-280*$^{-/-}$ mutants (Figure 4D). We conclude, that neuronal Tbx3 expression gradually declines during development and becomes undetectable at late fetal stages.

Electrophysiological characteristics of MT-280 mutants

Because *MT-280*$^{-/-}$ mutants exhibit embryonic lethality, we isolated hearts from E15.5 fetuses to measure atrial activation using local electrocardiograms. Heart rate was not statistically different between WT (n=5), *MT-280*$^{+/-}$ (n=13) and *MT-280*$^{-/-}$ (n=9) mutants (Figure 5A). ECG recordings from adult *MT-280*$^{+/-}$ mutants, which do survive into adulthood, revealed a slightly slower heart rate (increased RR interval) between WT (n=8) and *MT-280*$^{+/-}$ (n=13) mice *in vivo* (Figure 5B; Suppl. Fig. XI). Administration of atropine and propranolol to block the ANS caused heart rate decrease in both WT (n=7) and mutant mice (n=13). The decrease in heart rate was significantly larger in mutants compared to WT (Figure 5B,C). Furthermore, heart rate variability was significantly higher in *MT-280*$^{+/-}$ mice compared to WT, but this difference was lost after blocking ANS function (Figure 5B and Suppl. Fig. XI). We next applied overdrive suppression of the SAN by pacing the right atrium to investigate whether SAN recovery time was affected. We observed prolonged SAN recovery times in *MT-280*$^{+/-}$ mice compared to WT (Figure 5B and Suppl. Fig. XI) at 100 ms and 120 ms stimulation cycles. ANS block did not neutralize this difference between genotypes when tested at equivalent 120 ms and 140 ms cycle length, suggesting this property is affected in mutants independent of ANS function, and therefore likely intrinsic to SAN function. Other ECG parameters, including PR-interval, Wenkebach cycle length, and QRS-duration were not different between genotypes (Suppl. Fig. XI). We also tested whether atrial fibrillation (AF) could be induced. In both WT (n=13) and *MT-280*$^{+/-}$ (n=11) mice we found AF episodes of <10 sec and >10 sec that were not statistically different between genotypes (Suppl. Fig. XIB). We conclude that heterozygous deletion of *MT-280* affects heart rate variability in adult mice in an ANS dependent manner, and increases both RR interval duration and SAN recovery times independent of ANS function. Patch clamp analysis of single SAN pacemaker cardiomyocytes of WT and *MT-280*$^{+/}$ mice revealed that the action potential (AP) characteristics were not different between the genotypes (Suppl. Fig. XID,E).

Functionality assessment of REs in the *TBX3* locus

To identify REs involved in the regulation of *TBX3* expression in the SAN, we selected SANLPC-accessible DNA sites in the MT-280 region of the human genome (Figure 6A) and performed functional enhancer assays *in vivo*. We found *TBX3-RE2* to be functionally active in the Hcn4+ SAN of E11.5, in the limbs and, to a lesser extent, in the atrioventricular canal (Figure 6B). *TBX3-RE1–2*, a ±5 kb fragment covering two peaks, is located in a haploblock harboring multiple HRRAE SNPs, including the leading SNP rs61928421 (Figure 6C).[19, 20] Furthermore, these regions were also accessible in the genome of Hcn4$^+$ SAN cells in mice (Suppl. Fig. IB and VI). We first tested *TBX3-RE1–2* in transgenic mouse embryos and found that its activity was restricted to the heart (Figure 6D, Suppl. Fig. XIIA). Histological sectioning revealed robust activation of reporter gene expression in SANs of E10.5 embryos (5/7) (Figure 6D, Suppl. Fig. XIIA). In addition, in 5 of 7 independently generated F0 embryos we also observed activity in the atrioventricular canal in a pattern similar to *Tbx3* expression. We did not observe chromatin accessibility at the region harboring lead SNP rs61928421. Therefore, we investigated whether SNPs located in *TBX3-RE1–2* are in linkage disequilibrium (LD) with the leading SNP. High LD score (R^2=0.90) was found for rs140828160 (T=0.914; *gap*=0.086) in *TBX3-RE2* (Figure 6C). Next, we tested the functional activity of the minor allele variant of *TBX3-RE1–2* (±5 kb) and observed a heterogeneous, less robust activity pattern in the SAN in 2 of 7 independently generated F0 embryos at E10.5 (Figure 6D, Suppl. Fig. XIIB). We conclude that a distal region in the *TBX3* locus is necessary for *Tbx3* expression in the SAN and harbors REs functionally active in the SAN that could be affected by common genetic variants associated with HRRAE.

Discussion

Regulation of tissue-specific gene transcription is mediated by REs that are bound by tissue-specific TFs. Although multiple human cardiac REs have been identified,[14, 15] REs involved in SAN-specific gene regulation have not been described and functionally validated previously. In this study, we compared genome-wide chromatin accessibility profiles of human stem cell-derived SANLPC, as proxy for human (SAN) pacemaker cardiomyocytes, with those of VLCMs and of adult LA cardiomyocytes, respectively, to identify pacemaker cell-specific accessible sites. DNA accessibility is generally associated with regulatory element activity (including deployed enhancers) and suitable to identify TF binding sites.[22, 44] Using ATAC-seq, we thus identified thousands of putative pacemaker-specific REs and enriched TF binding motifs. The function of an accessible site, however, remains unknown. Less than half of the candidates REs that we tested in fish or mouse were found to drive pacemaker-specific reporter gene expression, indicating accessibility by itself is not sufficient to identify regulatory elements that function as autonomous enhancers.[45] Accessible sites may also function as repressors, only function in context (e.g. cooperatively with other elements), or function to regulate chromatin structure. Therefore, we provide a genome-wide collection of putative human REs, a subpopulation of which acts as pacemaker-specific enhancer.

Analysis of TF motifs in the accessible site populations identified predictable sites in each subpopulation, indicating the RE identification was specific. Thus, the hESC-specific subpopulation was associated with motifs for pluripotency TFs[46] and the subpopulation shared between SANPLC and VLCM (cardiomyocyte) was associated with Mef2 and Tead binding motifs.[47] In the VLCM-specific subpopulation of accessible sites, AP-1 (Jun/Fos) was highly enriched, suggesting AP-1 may be involved in the regulation of VLCM REs, but not of SANLPC REs. In the SANLPC-specific sites, motifs for Isl1, TALE homeobox (Meis1, Tgif1/2), T-Box and Gata TFs were identified. Consistently, Isl1, Tbx3, Tbx5 and Tbx18 are involved in pacemaker development and gene regulation in mouse and fish.[4, 7, 27, 39, 48] Little is known about the function of TALE homeobox proteins in pacemaker cell development or gene regulation. Meis1 is involved in the regulation of the cell cycle in cardiomyocytes, and both Meis1 and Meis2 and Tgif1 regulate cardiac neural crest cell development and outflow tract morphogenesis.[28–31, 49] Our data suggest these TFs may be involved in SAN pacemaker gene regulation. Smad motifs were also enriched in the SANLPC-specific accessible sites. The role of BMP-signaling (Smad) in the SAN is not well defined, although both human and mouse SANs and SANLPCs specifically express BMP2/4 (Figure 1A).[11] However, pacemaker-like cells of the atrioventricular canal/node are specified under control of BMP-signaling and Gata4/6,[50–54] suggesting that these regulatory mechanisms may act through SANLPC-specific REs as well.

TBX3 REs identified thus far were found to activate transcription in most tissues expressing *Tbx3*, including the atrioventricular conduction system,[42, 43] limbs, body wall, mammary glands and gonads,[33, 42, 43] but never in the SAN. These REs are located in relative close proximity (up to 100 kbp) to *Tbx3* in mice.[33, 43] Consistently, the majority of genetic variants associated with PR-interval[55] and QRS duration in the *TBX3* locus, reflecting atrioventricular conduction system function, has been detected in the regions harboring these atrioventricular REs. Here, we have identified the REs for SAN expression in the gene desert far upstream (±1 Mbp) of *TBX3*, close to *MED13L*. Homozygous deletion of this distal region from the mouse genome abolished *Tbx3* expression from the SAN in mice, whereas *Tbx3* expression was maintained in most other tissues, including the atrioventricular conduction system. Moreover, expression of *Tbx5* and *Med13l*, flanking *Tbx3* and potentially targeted by the REs in the deleted region, was not affected. Consistent with a specific role in *Tbx3* regulation, this distal region shares the TAD with TBX3, and previous 4C-seq and HiC-seq data indicated it is in close physical proximity to the promoter of *TBX3*.[43]

The human orthologous regions of mouse *MT-280* and *MT-550* harbor HRRAE-associated genetic variants. Because of their proximity to *MED13L*, these HRRAE variants were suggested to affect *MED13L* regulation.[20] However, our data indicate that *TBX3*, not *MED13L*, is the actual target of the variant REs in this associated region. Although absence of *Tbx3* from the SAN in fetal homozygous deletion mutants did not affect heart rate, heterozygous adult mutant mice exhibited slightly slower heart rates, more heart rate variability and prolonged SAN recovery times after pacing. These data are consistent with an effect of HRRAE-associated variants on *TBX3* expression in the SAN region of humans, although other causes of prolonged SAN recovery times than exercise cannot be excluded. *Tbx3* levels were also reduced in neurons and cardiac ganglia innervating the SAN (the ANS) in homozygous deletion mutant mice. Moreover, while decreased heart rates and increased SAN recovery times in heterozygous mutants were not neutralized by blocking ANS function, heart rate variability was. Our data thus suggest that reduction of *Tbx3* expression in mutants functionally affects both ANS and SAN pacemaker cells or their interaction.

Supplementary Material

Refer to Web version on PubMed Central for supplementary material.

Acknowledgements

We would like to thank Berend de Jonge for isolating SAN cells and performing patch clamp experiments.

Sources of funding

This study was supported by Netherlands Scientific Organization (ZonMW TOP 40-00812-98-12086), Leducq Foundation grant (14CVD01) and Dutch Heart Foundation (2013T091) to VMC. BJB received support from the Dutch Heart Foundation (2016T047) and Auriane Ernault from the FRM (Fondation pour la Recherche Médicale) (PBR201810007613). MDW is supported by the Canada Research Chairs Program. Work in the Black Lab performed in these studies was supported by NIH grants HL064658 and HL136182 to BLB.

Non-standard Abbreviations and Acronyms:

hESC	human embryonic stem cell
HRRAE	heart rate recovery after exercise
HRV	Heart rate variation
RE	regulatory element
SANLPC	sinoatrial node-like pacemaker cells
cSNRT	corrected sinus node recovery time
TF	transcription factor
TAD	topologically associating domains
VLCM	ventricle-like cardiomyocyte

References

1. Dobrzynski H, Boyett MR and Anderson RH. New insights into pacemaker activity: promoting understanding of sick sinus syndrome. Circulation 2007;115:1921–1932. [PubMed: 17420362]
2. van Eif VWW, Devalla HD, Boink GJJ and Christoffels VM. Transcriptional regulation of the cardiac conduction system. Nat Rev Cardiol 2018;15:1–14. [PubMed: 29188810]
3. Bhattacharyya S and Munshi NV. Development of the Cardiac Conduction System. Cold Spring Harbor perspectives in biology 2020.

4. Liang X, Zhang Q, Cattaneo P, Zhuang S, Gong X, Spann NJ, Jiang C, Cao X, Zhao X, Zhang X, Bu L, Wang G, Chen HS, Zhuang T, Yan J, Geng P, Luo L, Banerjee I, Chen Y, Glass CK, Zambon AC, Chen J, Sun Y and Evans SM. Transcription factor ISL1 is essential for pacemaker development and function. J Clin Invest 2015;125:3256–68. [PubMed: 26193633]
5. Blaschke RJ, Hahurij ND, Kuijper S, Just S, Wisse LJ, Deissler K, Maxelon T, Anastassiadis K, Spitzer J, Hardt SE, Scholer H, Feitsma H, Rottbauer W, Blum M, Meijlink F, Rappold G and Gittenberger-de Groot AC. Targeted mutation reveals essential functions of the homeodomain transcription factor Shox2 in sinoatrial and pacemaking development. Circulation 2007;115:1830–1838. [PubMed: 17372176]
6. Espinoza-Lewis RA, Yu L, He F, Liu H, Tang R, Shi J, Sun X, Martin JF, Wang D, Yang J and Chen Y. Shox2 is essential for the differentiation of cardiac pacemaker cells by repressing Nkx2–5. DevBiol 2009;327:378–385.
7. Hoogaars WM, Engel A, Brons JF, Verkerk AO, de Lange FJ, Wong LY, Bakker ML, Clout DE, Wakker V, Barnett P, Ravesloot JH, Moorman AF, Verheijck EE and Christoffels VM. Tbx3 controls the sinoatrial node gene program and imposes pacemaker function on the atria. Genes Dev 2007;21:1098–1112. [PubMed: 17473172]
8. Long HK, Prescott SL and Wysocka J. Ever-Changing Landscapes: Transcriptional Enhancers in Development and Evolution. Cell 2016;167:1170–1187. [PubMed: 27863239]
9. Furlong EEM and Levine M. Developmental enhancers and chromosome topology. Science 2018;361:1341–1345. [PubMed: 30262496]
10. Vedantham V, Galang G, Evangelista M, Deo RC and Srivastava D. RNA sequencing of mouse sinoatrial node reveals an upstream regulatory role for Islet-1 in cardiac pacemaker cells. Circ Res 2015;116:797–803. [PubMed: 25623957]
11. van Eif VWW, Stefanovic S, van Duijvenboden K, Bakker M, Wakker V, de Gier-de Vries C, Zaffran S, Verkerk AO, Boukens BJ and Christoffels VM. Transcriptome analysis of mouse and human sinoatrial node cells reveals a conserved genetic program. Development 2019;146:1–15.
12. Goodyer WR, Beyersdorf BM, Paik DT, Tian L, Li G, Buikema JW, Chirikian O, Choi S, Venkatraman S, Adams EL, Tessier-Lavigne M, Wu JC and Wu SM. Transcriptomic Profiling of the Developing Cardiac Conduction System at Single-Cell Resolution. Circ Res 2019;125:379–397. [PubMed: 31284824]
13. Linscheid N, Logantha S, Poulsen PC, Zhang S, Schrolkamp M, Egerod KL, Thompson JJ, Kitmitto A, Galli G, Humphries MJ, Zhang H, Pers TH, Olsen JV, Boyett M and Lundby A. Quantitative proteomics and single-nucleus transcriptomics of the sinus node elucidates the foundation of cardiac pacemaking. Nature communications 2019;10:2889.
14. Dickel DE, Barozzi I, Zhu Y, Fukuda-Yuzawa Y, Osterwalder M, Mannion BJ, May D, Spurrell CH, Plajzer-Frick I, Pickle CS, Lee E, Garvin TH, Kato M, Akiyama JA, Afzal V, Lee AY, Gorkin DU, Ren B, Rubin EM, Visel A and Pennacchio LA. Genome-wide compendium and functional assessment of in vivo heart enhancers. Nature communications 2016;7:12923.
15. van Ouwerkerk AF, Bosada FM, van Duijvenboden K, Hill MC, Montefiori LE, Scholman KT, Liu J, de Vries AAF, Boukens BJ, Ellinor PT, Goumans M, Efimov IR, Nobrega MA, Barnett P, Martin JF and Christoffels VM. Identification of atrial fibrillation associated genes and functional non-coding variants. Nature communications 2019;10:4755.
16. Liang X, Evans SM and Sun Y. Development of the cardiac pacemaker. Cell Mol Life Sci 2017;74:1247–1259. [PubMed: 27770149]
17. Birket MJ, Ribeiro MC, Verkerk AO, Ward D, Leitoguinho AR, den Hartogh SC, Orlova VV, Devalla HD, Schwach V, Bellin M, Passier R and Mummery CL. Expansion and patterning of cardiovascular progenitors derived from human pluripotent stem cells. Nat Biotechnol 2015;33:970–981. [PubMed: 26192318]
18. Protze SI, Liu J, Nussinovitch U, Ohana L, Backx PH, Gepstein L and Keller GM. Sinoatrial node cardiomyocytes derived from human pluripotent cells function as a biological pacemaker. Nat Biotechnol 2017;35:56–68. [PubMed: 27941801]
19. Ramirez J, Duijvenboden SV, Ntalla I, Mifsud B, Warren HR, Tzanis E, Orini M, Tinker A, Lambiase PD and Munroe PB. Thirty loci identified for heart rate response to exercise and recovery implicate autonomic nervous system. Nature communications 2018;9:1947.

20. Verweij N, van de Vegte YJ and van der Harst P. Genetic study links components of the autonomous nervous system to heart-rate profile during exercise. Nature communications 2018;9:898.
21. Elliott DA, Braam SR, Koutsis K, Ng ES, Jenny R, Lagerqvist EL, Biben C, Hatzistavrou T, Hirst CE, Yu QC, Skelton RJ, Ward-van Oostwaard D, Lim SM, Khammy O, Li X, Hawes SM, Davis RP, Goulburn AL, Passier R, Prall OW, Haynes JM, Pouton CW, Kaye DM, Mummery CL, Elefanty AG and Stanley EG. NKX2–5(eGFP/w) hESCs for isolation of human cardiac progenitors and cardiomyocytes. NatMethods 2011;8:1037–1040.
22. Buenrostro JD, Giresi PG, Zaba LC, Chang HY and Greenleaf WJ. Transposition of native chromatin for fast and sensitive epigenomic profiling of open chromatin, DNA-binding proteins and nucleosome position. Nature methods 2013;10:1213–8. [PubMed: 24097267]
23. Li QV, Dixon G, Verma N, Rosen BP, Gordillo M, Luo R, Xu C, Wang Q, Soh CL, Yang D, Crespo M, Shukla A, Xiang Q, Dundar F, Zumbo P, Witkin M, Koche R, Betel D, Chen S, Massague J, Garippa R, Evans T, Beer MA and Huangfu D. Genome-scale screens identify JNK-JUN signaling as a barrier for pluripotency exit and endoderm differentiation. Nat Genet 2019;51:999–1010. [PubMed: 31110351]
24. Zhang M, Hill MC, Kadow ZA, Suh JH, Tucker NR, Hall AW, Tran TT, Swinton PS, Leach JP, Margulies KB, Ellinor PT, Li N and Martin JF. Long-range Pitx2c enhancer-promoter interactions prevent predisposition to atrial fibrillation. Proc Natl Acad Sci U S A 2019;116:22692–22698. [PubMed: 31636200]
25. Rao SS, Huntley MH, Durand NC, Stamenova EK, Bochkov ID, Robinson JT, Sanborn AL, Machol I, Omer AD, Lander ES and Aiden EL. A 3D map of the human genome at kilobase resolution reveals principles of chromatin looping. Cell 2014;159:1665–80. [PubMed: 25497547]
26. van Duijvenboden K, de Boer BA, Capon N, Ruijter JM and Christoffels VM. EMERGE: a flexible modelling framework to predict genomic regulatory elements from genomic signatures. Nucleic Acids Res 2015;44.
27. Mori AD, Zhu Y, Vahora I, Nieman B, Koshiba-Takeuchi K, Davidson L, Pizard A, Seidman CE, Seidman JG, Chen XJ, Henkelman RM and Bruneau BG. Tbx5-dependent rheostatic control of cardiac gene expression and morphogenesis. Dev Biol 2006;297:566–586. [PubMed: 16870172]
28. Machon O, Masek J, Machonova O, Krauss S and Kozmik Z. Meis2 is essential for cranial and cardiac neural crest development. BMC developmental biology 2015;15:40. [PubMed: 26545946]
29. Bouilloux F, Thireau J, Venteo S, Farah C, Karam S, Dauvilliers Y, Valmier J, Copeland NG, Jenkins NA, Richard S and Marmigere F. Loss of the transcription factor Meis1 prevents sympathetic neurons target-field innervation and increases susceptibility to sudden cardiac death. Elife 2016;5.
30. Nguyen NUN, Canseco DC, Xiao F, Nakada Y, Li S, Lam NT, Muralidhar SA, Savla JJ, Hill JA, Le V, Zidan KA, El-Feky HW, Wang Z, Ahmed MS, Hubbi ME, Menendez-Montes I, Moon J, Ali SR, Le V, Villalobos E, Mohamed MS, Elhelaly WM, Thet S, Anene-Nzelu CG, Tan WLW, Foo RS, Meng X, Kanchwala M, Xing C, Roy J, Cyert MS, Rothermel BA and Sadek HA. A calcineurin-Hoxb13 axis regulates growth mode of mammalian cardiomyocytes. Nature 2020;582:271–276. [PubMed: 32499640]
31. Gandhi S, Ezin M and Bronner ME. Reprogramming Axial Level Identity to Rescue Neural-Crest-Related Congenital Heart Defects. Dev Cell 2020;53:300–315 e4. [PubMed: 32369742]
32. Fernandez-Perez A, Sathe AA, Bhakta M, Leggett K, Xing C and Munshi NV. Hand2 Selectively Reorganizes Chromatin Accessibility to Induce Pacemaker-like Transcriptional Reprogramming. Cell Rep 2019;27:2354–2369 e7. [PubMed: 31116981]
33. Osterwalder M, Barozzi I, Tissieres V, Fukuda-Yuzawa Y, Mannion BJ, Afzal SY, Lee EA, Zhu Y, Plajzer-Frick I, Pickle CS, Kato M, Garvin TH, Pham QT, Harrington AN, Akiyama JA, Afzal V, Lopez-Rios J, Dickel DE, Visel A and Pennacchio LA. Enhancer redundancy provides phenotypic robustness in mammalian development. Nature 2018;554:239–243. [PubMed: 29420474]
34. Hoffmann S, Berger IM, Glaser A, Bacon C, Li L, Gretz N, Steinbeisser H, Rottbauer W, Just S and Rappold G. Islet1 is a direct transcriptional target of the homeodomain transcription factor Shox2 and rescues the Shox2-mediated bradycardia. Basic ResCardiol 2013;108:339.
35. Ye W, Wang J, Song Y, Yu D, Sun C, Liu C, Chen F, Zhang Y, Wang F, Harvey RP, Schrader L, Martin JF and Chen Y. A common Shox2-Nkx2–5 antagonistic mechanism primes the pacemaker

cell fate in the pulmonary vein myocardium and sinoatrial node. Development 2015;142:2521–32. [PubMed: 26138475]

36. Mommersteeg MTM, Hoogaars WMH, Prall OWJ, de Gier-de Vries C, Wiese C, D.E.W. C, Papaioannou VE, Brown NA, Harvey RP, Moorman AFM and Christoffels VM. Molecular pathway for the localized formation of the sinoatrial node. CircRes 2007;100:354–362.
37. Li H, Li D, Wang Y, Huang Z, Xu J, Yang T, Wang L, Tang Q, Cai CL, Huang H, Zhang Y and Chen Y. Nkx2–5 defines a subpopulation of pacemaker cells and is essential for the physiological function of the sinoatrial node in mice. Development 2019;146.
38. Arrenberg AB, Stainier DY, Baier H and Huisken J. Optogenetic control of cardiac function. Science 2010;330:971–974. [PubMed: 21071670]
39. Tessadori F, van Weerd JH, Burkhard SB, Verkerk AO, de PE, Boukens BJ, Vink A, Christoffels VM and Bakkers J. Identification and functional characterization of cardiac pacemaker cells in zebrafish. PLoSONE 2012;7:e47644.
40. Sun C, Zhang T, Liu C, Gu S and Chen Y. Generation of Shox2-Cre allele for tissue specific manipulation of genes in the developing heart, palate, and limb. Genesis 2013;51:515–22. [PubMed: 23620086]
41. de Laat W and Duboule D. Topology of mammalian developmental enhancers and their regulatory landscapes. Nature 2013;502:499–506. [PubMed: 24153303]
42. Horsthuis T, Buermans HP, Brons JF, Verkerk AO, Bakker ML, Wakker V, Clout DE, Moorman AF, ‘t Hoen PA and Christoffels VM. Gene expression profiling of the forming atrioventricular node using a novel Tbx3-based node-specific transgenic reporter. CircRes 2009;105:61–69.
43. van Weerd JH, Badi I, van den Boogaard M, Stefanovic S, van de Werken HJ, Gomez-Velazquez M, Badia-Careaga C, Manzanares M, de Laat W, Barnett P and Christoffels VM. A Large Permissive Regulatory Domain Exclusively Controls Tbx3 Expression in the Cardiac Conduction System. CircRes 2014;115:432–441.
44. Thurman RE, Rynes E, Humbert R, Vierstra J, Maurano MT, Haugen E, Sheffield NC, Stergachis AB, Wang H, Vernot B, Garg K, John S, Sandstrom R, Bates D, Boatman L, Canfield TK, Diegel M, Dunn D, Ebersol AK, Frum T, Giste E, Johnson AK, Johnson EM, Kutyavin T, Lajoie B, Lee BK, Lee K, London D, Lotakis D, Neph S, Neri F, Nguyen ED, Qu H, Reynolds AP, Roach V, Safi A, Sanchez ME, Sanyal A, Shafer A, Simon JM, Song L, Vong S, Weaver M, Yan Y, Zhang Z, Zhang Z, Lenhard B, Tewari M, Dorschner MO, Hansen RS, Navas PA, Stamatoyannopoulos G, Iyer VR, Lieb JD, Sunyaev SR, Akey JM, Sabo PJ, Kaul R, Furey TS, Dekker J, Crawford GE and Stamatoyannopoulos JA. The accessible chromatin landscape of the human genome. Nature 2012;489:75–82. [PubMed: 22955617]
45. Hsiung CC, Morrissey CS, Udugama M, Frank CL, Keller CA, Baek S, Giardine B, Crawford GE, Sung MH, Hardison RC and Blobel GA. Genome accessibility is widely preserved and locally modulated during mitosis. Genome research 2015;25:213–25. [PubMed: 25373146]
46. Boyer LA, Lee TI, Cole MF, Johnstone SE, Levine SS, Zucker JP, Guenther MG, Kumar RM, Murray HL, Jenner RG, Gifford DK, Melton DA, Jaenisch R and Young RA. Core transcriptional regulatory circuitry in human embryonic stem cells. Cell 2005;122:947–956. [PubMed: 16153702]
47. Akerberg BN, Gu F, VanDusen NJ, Zhang X, Dong R, Li K, Zhang B, Zhou B, Sethi I, Ma Q, Wasson L, Wen T, Liu J, Dong K, Conlon FL, Zhou J, Yuan GC, Zhou P and Pu WT. A reference map of murine cardiac transcription factor chromatin occupancy identifies dynamic and conserved enhancers. Nature communications 2019;10:4907.
48. Wiese C, Grieskamp T, Airik R, Mommersteeg MT, Gardiwal A, de Gier-de VC, Schuster-Gossler K, Moorman AF, Kispert A and Christoffels VM. Formation of the sinus node head and differentiation of sinus node myocardium are independently regulated by tbx18 and tbx3. CircRes 2009;104:388–397.
49. Stankunas K, Shang C, Twu KY, Kao SC, Jenkins NA, Copeland NG, Sanyal M, Selleri L, Cleary ML and Chang CP. Pbx/Meis deficiencies demonstrate multigenetic origins of congenital heart disease. CircRes 2008;103:702–709.
50. Ma L, Lu MF, Schwartz RJ and Martin JF. Bmp2 is essential for cardiac cushion epithelial-mesenchymal transition and myocardial patterning. Development 2005;132:5601–5611. [PubMed: 16314491]

51. Munshi NV, McAnally J, Bezprozvannaya S, Berry JM, Richardson JA, Hill JA and Olson EN. Cx30.2 enhancer analysis identifies Gata4 as a novel regulator of atrioventricular delay. Development 2009;136:2665–2674. [PubMed: 19592579]

52. Stefanovic S, Barnett P, van Duijvenboden K, Weber D, Gessler M and Christoffels VM. GATA-dependent regulatory switches establish atrioventricular canal specificity during heart development. NatCommun 2014;5:3680.

53. Liu F, Lu MM, Patel NN, Schillinger KJ, Wang T and Patel VV. GATA-Binding Factor 6 Contributes to Atrioventricular Node Development and Function. Circulation Cardiovascular genetics 2015;8:284–93. [PubMed: 25613430]

54. Verhoeven MC, Haase C, Christoffels VM, Weidinger G and Bakkers J. Wnt signaling regulates atrioventricular canal formation upstream of BMP and Tbx2. Birth Defects ResA ClinMolTeratol 2011;91:435–440.

55. van Setten J, Brody JA, Jamshidi Y, Swenson BR, Butler AM, Campbell H, Del Greco FM, Evans DS, Gibson Q, Gudbjartsson DF, Kerr KF, Krijthe BP, Lyytikainen LP, Muller C, Muller-Nurasyid M, Nolte IM, Padmanabhan S, Ritchie MD, Robino A, Smith AV, Steri M, Tanaka T, Teumer A, Trompet S, Ulivi S, Verweij N, Yin X, Arnar DO, Asselbergs FW, Bader JS, Barnard J, Bis J, Blankenberg S, Boerwinkle E, Bradford Y, Buckley BM, Chung MK, Crawford D, den Hoed M, Denny JC, Dominiczak AF, Ehret GB, Eijgelsheim M, Ellinor PT, Felix SB, Franco OH, Franke L, Harris TB, Holm H, Ilaria G, Iorio A, Kahonen M, Kolcic I, Kors JA, Lakatta EG, Launer LJ, Lin H, Lin HJ, Loos RJF, Lubitz SA, Macfarlane PW, Magnani JW, Leach IM, Meitinger T, Mitchell BD, Munzel T, Papanicolaou GJ, Peters A, Pfeufer A, Pramstaller PP, Raitakari OT, Rotter JI, Rudan I, Samani NJ, Schlessinger D, Silva Aldana CT, Sinner MF, Smith JD, Snieder H, Soliman EZ, Spector TD, Stott DJ, Strauch K, Tarasov KV, Thorsteinsdottir U, Uitterlinden AG, Van Wagoner DR, Volker U, Volzke H, Waldenberger M, Jan Westra H, Wild PS, Zeller T, Alonso A, Avery CL, Bandinelli S, Benjamin EJ, Cucca F, Dorr M, Ferrucci L, Gasparini P, Gudnason V, Hayward C, Heckbert SR, Hicks AA, Jukema JW, Kaab S, Lehtimaki T, Liu Y, Munroe PB, Parsa A, Polasek O, Psaty BM, Roden DM, Schnabel RB, Sinagra G, Stefansson K, Stricker BH, van der Harst P, van Duijn CM, Wilson JF, Gharib SA, de Bakker PIW, Isaacs A, Arking DE and Sotoodehnia N. PR interval genome-wide association meta-analysis identifies 50 loci associated with atrial and atrioventricular electrical activity. Nature communications 2018;9:2904.

56. Moorman AFM, Houweling AC, de Boer PAJ and Christoffels VM. Sensitive nonradioactive detection of mRNA in tissue sections: novel application of the whole-mount in situ hybridization protocol. JHistochemCytochem 2001;49:1–8.

57. Ruijter JM, Ramakers C, Hoogaars WM, Karlen Y, Bakker O, van den Hoff MJ and Moorman AF. Amplification efficiency: linking baseline and bias in the analysis of quantitative PCR data. Nucleic Acids Res 2009;37:e45. [PubMed: 19237396]

58. Jumrussirikul P, Dinerman J, Dawson TM, Dawson VL, Ekelund U, Georgakopoulos D, Schramm LP, Calkins H, Snyder SH, Hare JM and Berger RD. Interaction between neuronal nitric oxide synthase and inhibitory G protein activity in heart rate regulation in conscious mice. Journal of Clinical Investigation 1998;102:1279–1285.

59. Barry PH and Lynch JW. Liquid junction potentials and small cell effects in patch-clamp analysis. J Membr Biol 1991;121:101–17. [PubMed: 1715403]

60. Li H and Durbin R. Fast and accurate short read alignment with Burrows-Wheeler transform. Bioinformatics 2009;25:1754–60. [PubMed: 19451168]

61. Quinlan AR and Hall IM. BEDTools: a flexible suite of utilities for comparing genomic features. Bioinformatics 2010;26:841–2. [PubMed: 20110278]

62. Heinz S, Benner C, Spann N, Bertolino E, Lin YC, Laslo P, Cheng JX, Murre C, Singh H and Glass CK. Simple combinations of lineage-determining transcription factors prime cis-regulatory elements required for macrophage and B cell identities. Mol Cell 2010;38:576–89. [PubMed: 20513432]

Novelty and Significance

What is known?

- Lineage-specific transcription factors bind discrete genomic regions (regulatory elements) to control gene expression, cell differentiation and function.
- Regulatory elements can harbor (common) genetic variants that influence gene regulation and impact traits and diseases.
- A transcriptional regulatory network involving the lineage-specific transcription factors TBX3, SHOX2 and ISL1 controls sinoatrial node development and function.

What new information does this article contribute?

- We provide a genome-wide accessibility profile of human stem cell-derived pacemaker cells, identifying thousands of potential pacemaker-specific regulatory elements.
- Candidate human regulatory elements drive pacemaker-specific gene expression in vivo in transgenic mice and fish.
- Regulatory elements in the gene desert upstream of *TBX3* harbor heart rate recovery-associated SNPs and drive expression of *TBX3* in the sinoatrial node.

The development and function of the sinoatrial node, the principal pacemaker of the heart, is controlled by lineage-specific transcription factors, including SHOX2 and TBX3, bound to regulatory elements. Genetic variation in these regulatory elements can influence developmental and disease gene expression and phenotypes. However, such regulatory elements have not been identified for the sinoatrial node. Here, we provide the first genome-wide accessibility profile of human stem cell-derived sinoatrial node-like pacemaker cells, identifying thousands of potential pacemaker regulatory elements. Candidate elements discovered drove pacemaker-specific gene expression in transgenic mouse and fish embryos. Deletion of such elements from the mouse non-coding genome resulted in selective loss of SHOX2 or TBX3 expression, respectively, from the sinoatrial node and in lethality. We found a functional link between heart rate recovery-associated SNPs one million base pairs away from *TBX3* and a variant regulatory element driving sinoatrial node-specific expression. This work provides insight into the human sinoatrial node gene regulatory network and uncovers a mechanism underlying the influence of common human genetic variation on pacemaker function.

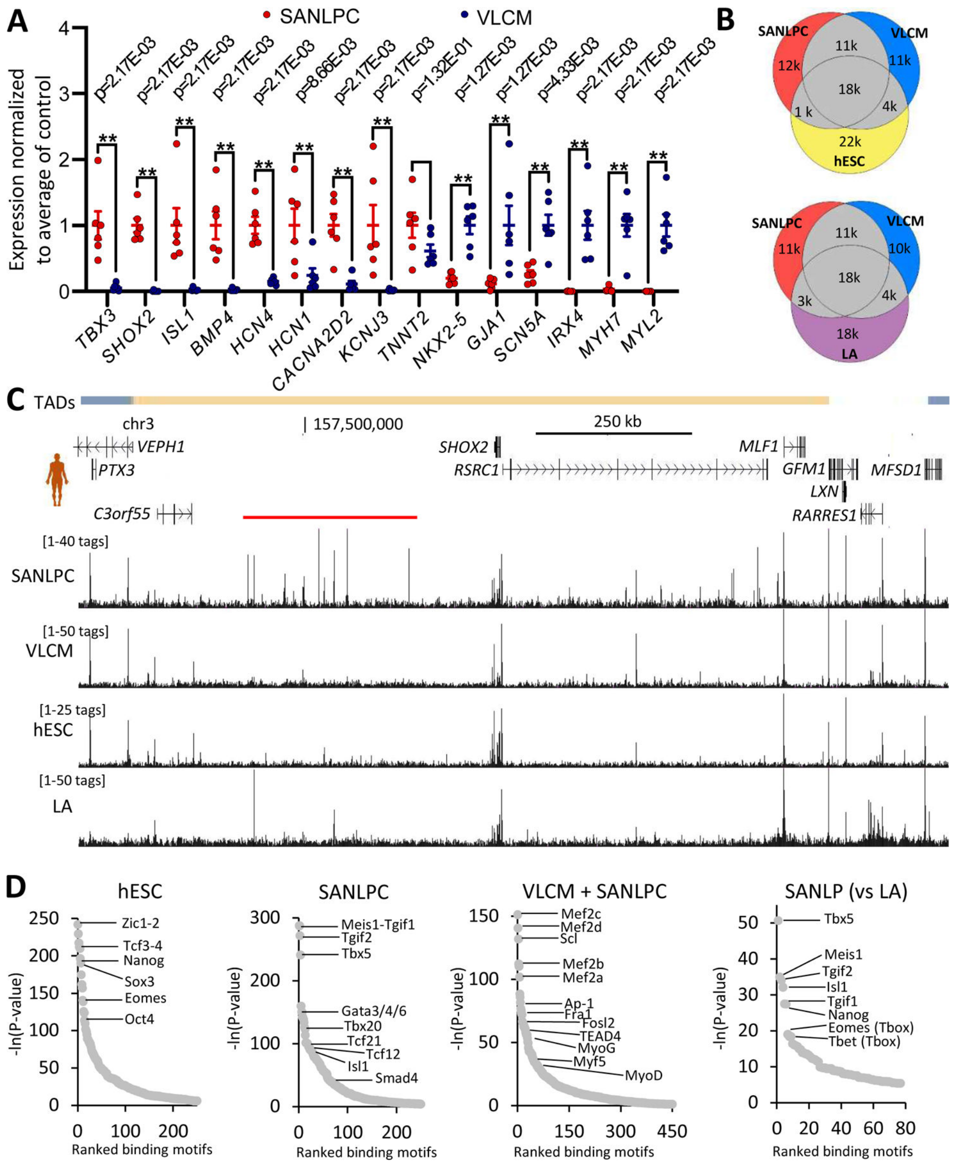

Figure 1.

Cell type validation and HOMER motif analysis of SANLPC and VLCM. (A) Expression levels of SAN and non-SAN genes in SANLPC (n=6) and VLCM (n=6). (B) Peak calling in SANLPC, VLCM, hESC and LA. (C) ATAC-sequencing revealed multiple accessible regions in the *SHOX2* locus in SANLPC only, indicated by red bar. Regions adjacent but in the TAD of *SHOX2* show similar accessibility profiles. (D) HOMER motif analysis on cell type-specific peaks in hESC, VLCM, SANLPC, VLCM+SANLPC and SANLPC vs LA. LA, left atrium.

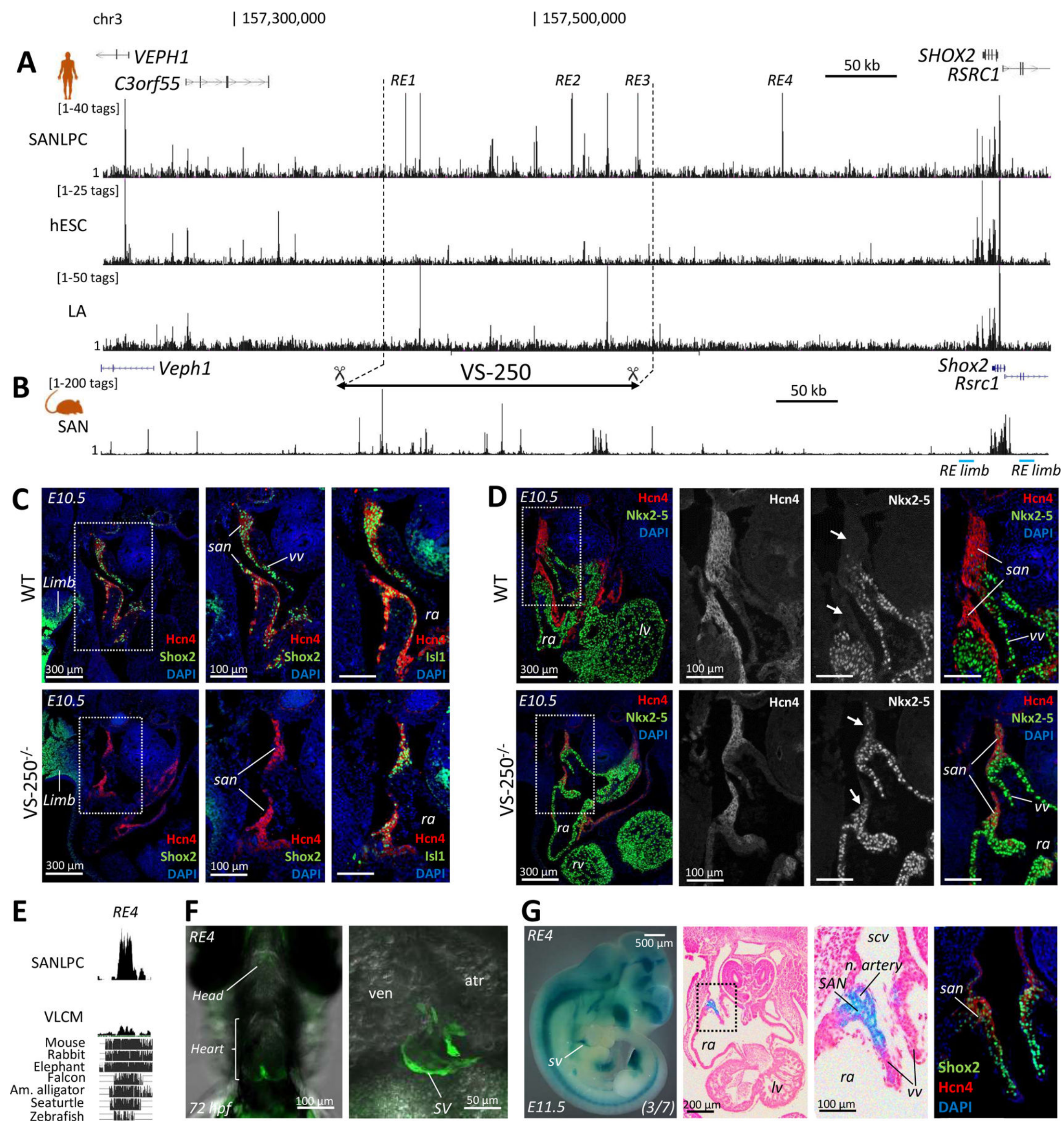

Figure 2.

Shox2 expression becomes depleted from the sinus venosus and SAN after deletion of regulatory elements. (A) ATAC-sequencing revealed multiple SANLPC-specific accessible regions in the *SHOX2* locus. (B) ATAC-track of purified Hcn4^{+} P0 SAN cells, showing accessible regions in the *Shox2* locus in mice. Region VS-250 was removed from the mouse genome, corresponding to the area indicated in 2A. (C) Immunostaining showing expression of *Shox2* and *Hcn4* in the sinus venosus region, including the SAN, in E10.5 wild type and *VS-250*$^{-/-}$ embryos (n=3). Expression of *Hcn4* and *Isl1* is maintained in the Shox2^{-} SAN. (D) Expression pattern of Nkx2–5 in the hearts and SAN of E10.5 wild type mice and *VS-250*$^{-/-}$ mutants. Arrows show activation of Nkx2–5 expression in the SAN of *VS-250*$^{-/-}$ embryos. Hypoplastic SANs and abnormal developed venous valves were observed for *VS-250*$^{-/-}$ mice. Region *SHOX2-RE4* was found to be deeply evolutionary conserved (E) and drove reporter expression in the sinus venosus of 72 hpf zebrafish (F) and in the SAN of

E11.5 mice, confirmed by immunohistochemical staining (G). a, atrium; v, ventricle; sv, sinus venosus; re, right atrium; rv, right ventricle; lv, left ventricle; san, sinoatrial node; vv, venous valves; scv, superior caval vein; n. artery, nodal artery.

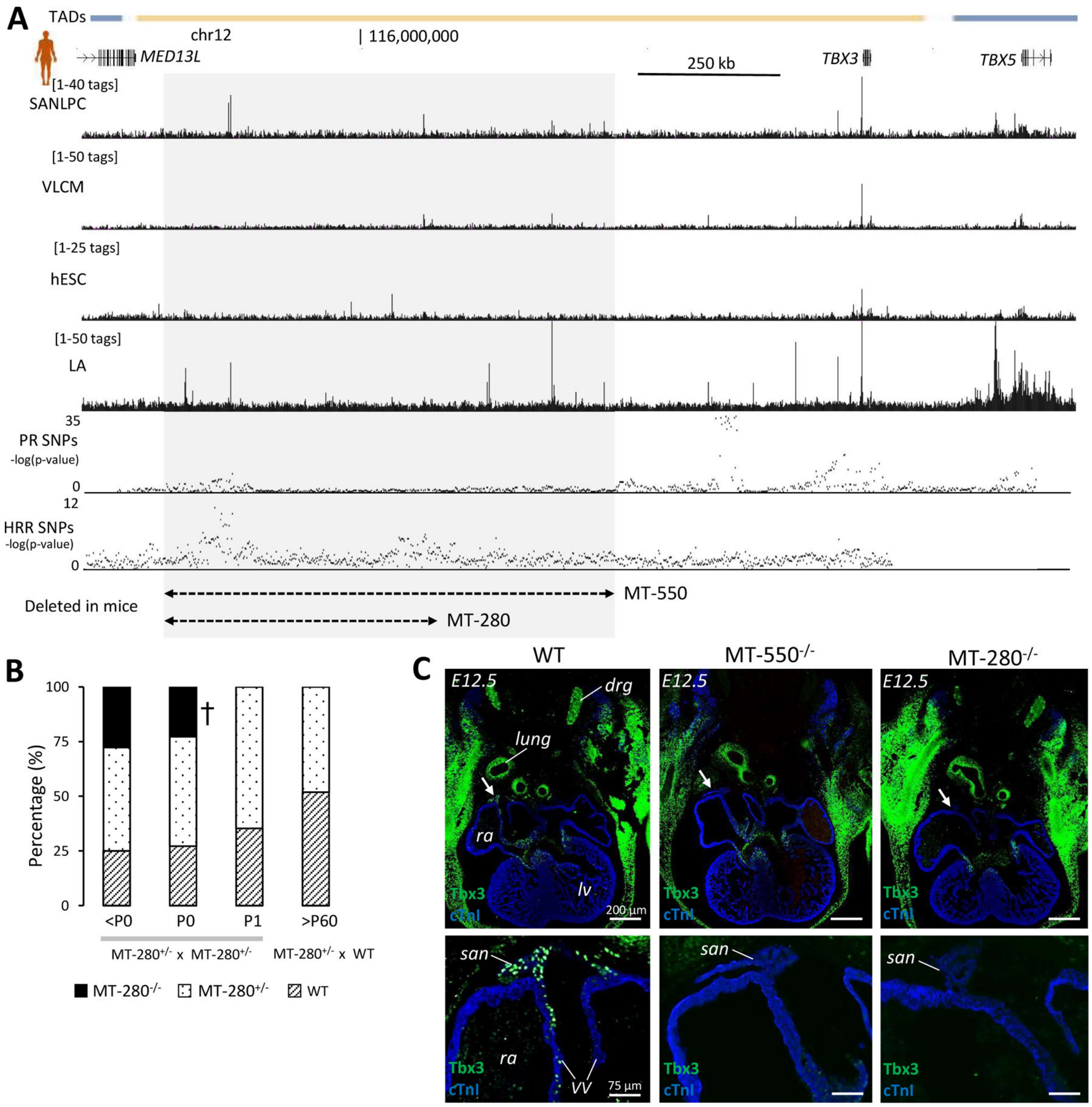

Figure 3.

Deletion of a region in the *Tbx3* locus associated with heart rate recovery abolished *Tbx3* expression in the SAN. (A) Accessible regions in the topologically-associating domain of TBX3. Genetic variants associated with heart rate recovery after exercise[20] and PR-interval[55] are shown. Regions corresponding to MT-280 and MT-550 were removed from the mouse genome. (B) Distribution of genotypes of litters, shown as percentages at a given developmental stage (<P0, before birth; P0; P1 and P60). *MT-280*$^{-/-}$ mutants die several hours after birth (cross), whereas *MT-280*$^{+/-}$ mice survive into adulthood and do not display different life expectancy. (C) Immunostaining of E12.5 wild type, *MT-280*$^{-/-}$ (n=3) and *MT-550*$^{-/-}$ embryos (n=6). Loss of Tbx3 expression was restricted to the SAN in homozygous mutants. HRR, heart rate recovery; PR, PR-interval; san, sinoatrial node; lv, left ventricle; ra, right atrium; vv, venous valves.

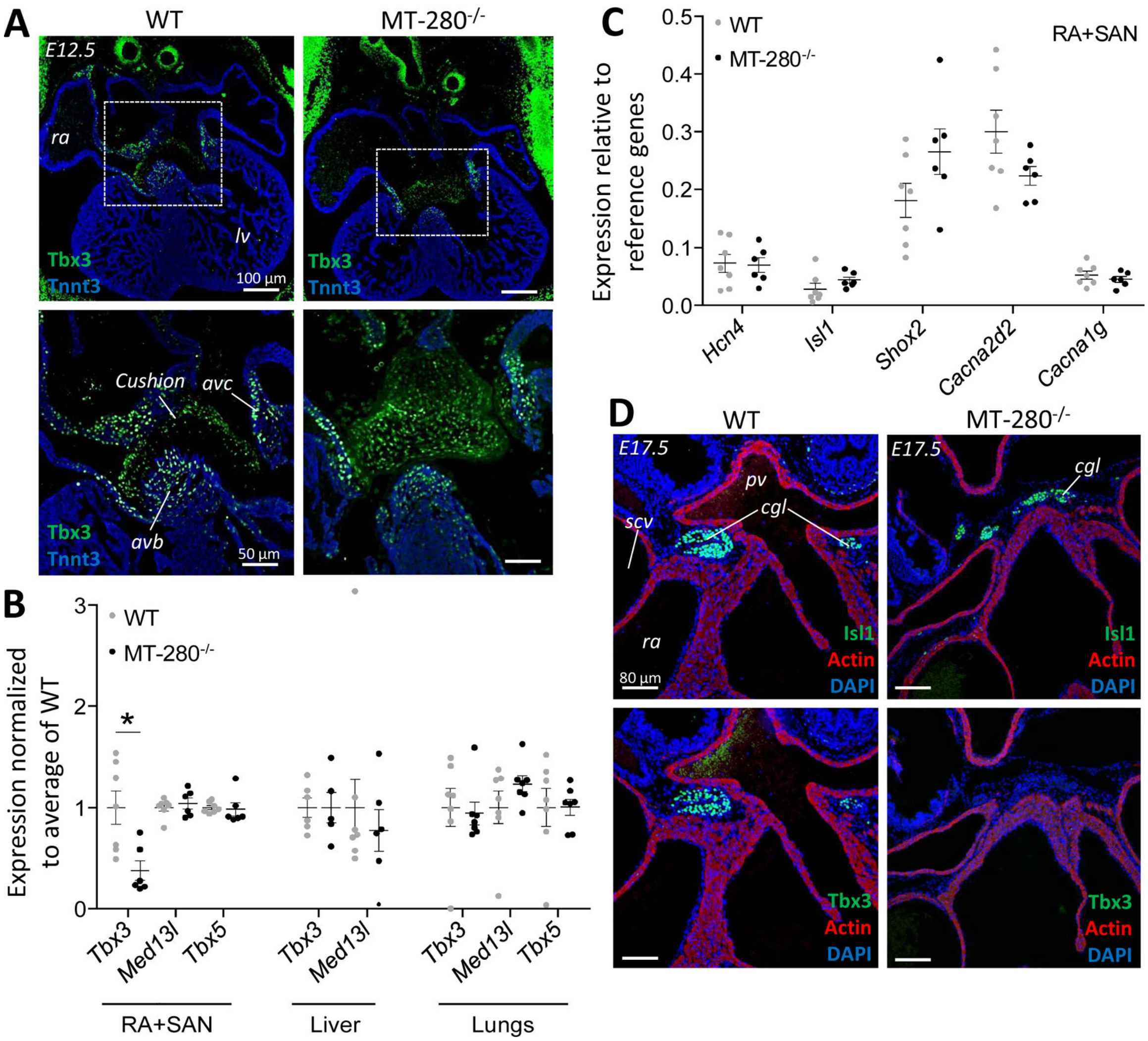

Figure 4.

Gene expression levels in body components after deletion of a distal non-coding region in the *Tbx3* locus. (A) Immunostaining showing maintenance of Tbx3 expression in the atrioventricular canal of homozygous mutants (n=3). (B) Relative expression levels of *Tbx3*, *Tbx5* and *Med13l* in E17.5 right atrium+SAN of wild type (n=7) and *MT-280*$^{-/-}$ (n=6), liver (wild type n=6; *MT-280*$^{-/-}$ n=5) and lung (wild type n=6; *MT-280*$^{-/-}$ n=7). (C) Relative expression levels of SAN genes in E17.5 right atrium+SAN samples of wild type (n=7) and *MT-280*$^{-/-}$ mutants (n=6). (D) *Tbx3* expression was absent in the cardiac ganglia, innervating the SAN, in E17.5 *MT-280*$^{-/-}$ fetuses. ra, right atrium; san, sinoatrial node; lv, left ventricle; avc, atrioventricular canal; avb, atrioventricular bundle; scv, superior caval vein; cgl, cardiac ganglion; pv, pulmonary vein.

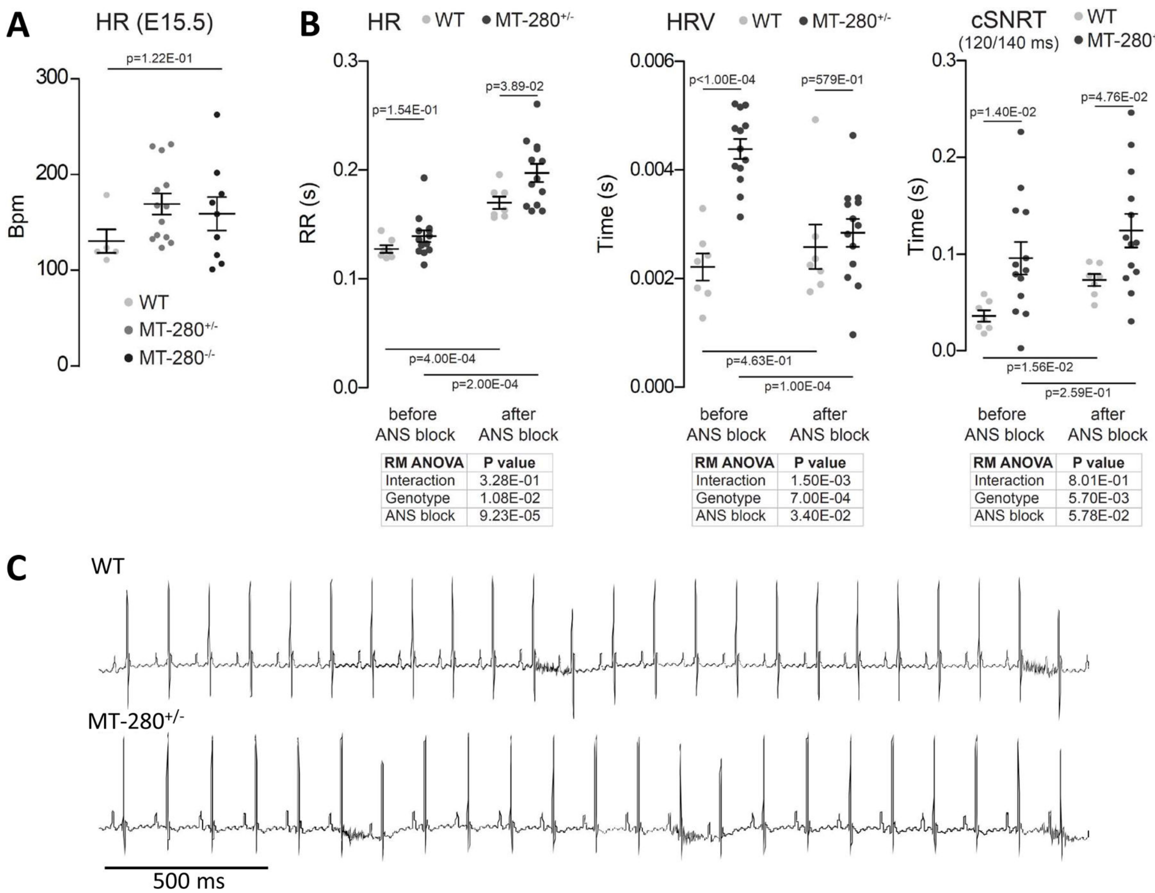

Figure 5.

Electrophysiological characteristics of *MT-280* mutant mice. (A) Heart rate was not significantly different between E15.5 WT (n=7), *MT-280*$^{+/-}$ (n=13) and *MT-280*$^{-/-}$ (n=9) fetuses by Kruskal-Wallis test. (B) *In vivo* ECG measurements and burst pacing of WT (n=7) and *MT-280*$^{+/-}$ mice (n=13) before and after ANS block. Tables denote repeated-measures ANOVA result. Within treatment groups, genotype differences were assessed using Student's t tests, and treatment differences within each genotype were assessed using paired t tests (pairwise p values shown within graph). (C) Example traces of ECGs of WT and *MT-280*$^{+/-}$ mice. HR, heart rate; ANS, autonomic nervous system; HRV, heart rate variability.

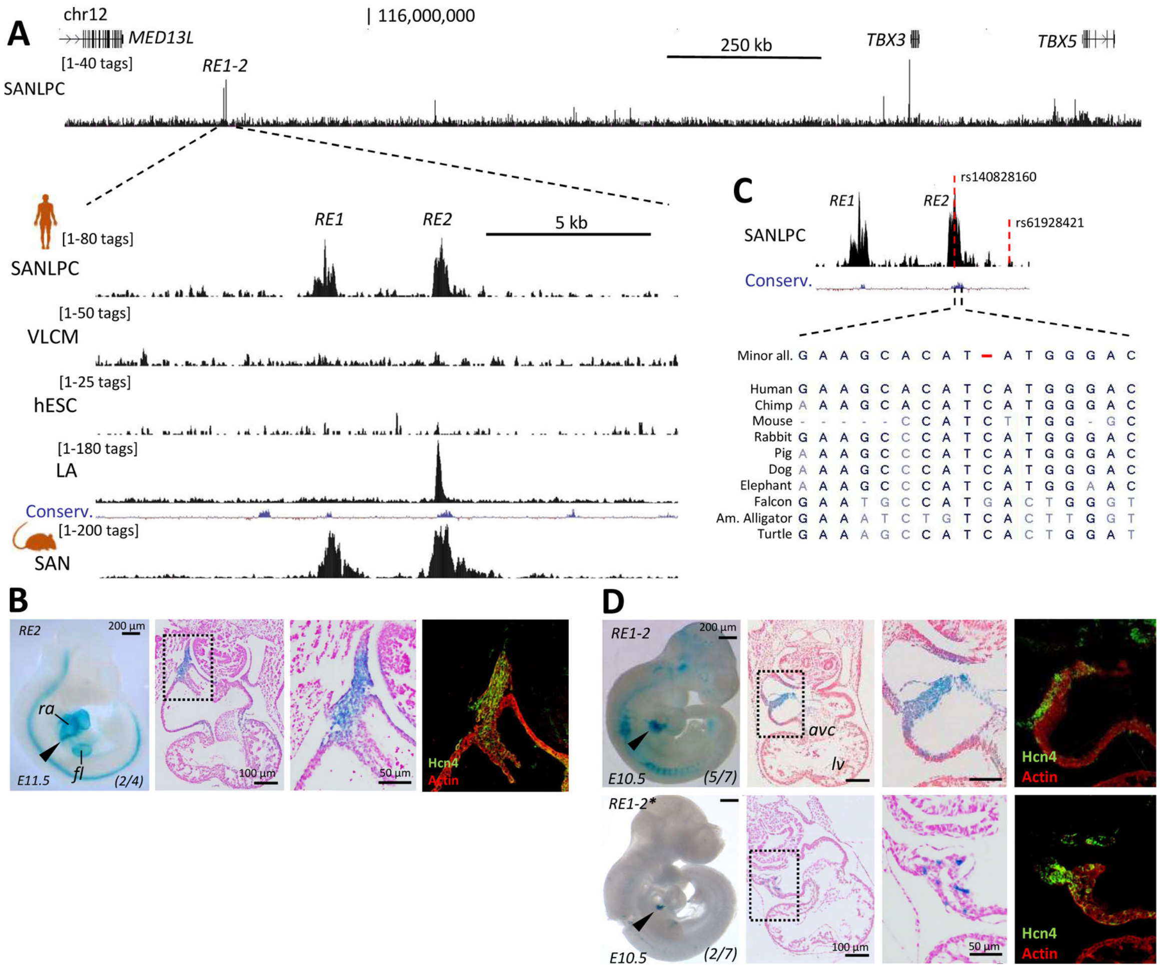

Figure 6.

Functional analysis of candidate REs in the *TBX3* locus. (A) Accessible regions in human SANLPC, VLCM, hESC and LA and mouse SAN harboring genetic variants associated with heart rate recovery after exercise. (B) Assessment of *TBX3-RE2 in vivo* revealed functional activity in the SAN, confirmed by immunostaining. (C) Position of genetic variant rs140828160, covering *TBX3-RE2,* and rs61928421, associated with heart rate recovery after exercise. (D) Both the major and minor allele variant of *TBX3-RE1–2* (±5 kb) were shown to be functionally active in the SAN of E11.5 mice, which was confirmed by immunolabeling. The minor allele variant is indicated by asterisk.